The 5th Asian Conference on Refrigeration and Air Conditioning
Proceedings of 5th ACRA
June 7-9, 2010, Tokyo, JAPAN

Paper No. 029

Modeling and Simulation of the Operation of a Rotary Magnetic Refrigerator

Didier VUARNOZ[*] Andrej KITANOVSKI[**] Cyrill GONIN[**]
Peter W. EGOLF[**] Tsuyoshi KAWANAMI [*]

*Department of Mechanical Engineering, Graduate School of Engineering, Kobe University
(1-1 Rokkodai-cho, Nada-ku, Kobe, 657-8501, Japan)

**Institute of Thermal Sciences and Engineering IGT, University of Applied Sciences of Western Switzerland
(Route de Cheseaux 1, 1401 Yverdon-les-Bains, Switzerland)

Summary

Magnetic refrigeration is a new environmentally benign technology and a promising alternative to conventional vapor-cycle refrigeration. The household refrigerator without a freezing compartment shows very good prospects for a successful application. This article starts with the general principle of magnetic refrigeration. An example of a magnet assembly is proposed and the corresponding magnetic flux lines are evaluated with a three-dimensional finite-element method (FEM). The maximum specific cooling capacity of magneto caloric materials is described. The specific cooling power of a magneto caloric material is found to be large even for medium magnetic field changes, especially if the frequency is not too small. For a domestic magnetic refrigerator, a comparison with a standard compressor refrigerator is presented. The modeling of a rotary magnetic refrigerator is described and its dynamic behavior is investigated. The physical model is based on a mapping of the magneto-thermodynamic problem from a cylinder onto two rectangles. In this model, in a basic centre cell, two coupled linear partial differential equations are solved, which have been programmed in the Modelica language. Steady-state solutions are envisaged to determine the coefficient of performance, *COP*, for these conditions. In future work the developed model shall be applied for an optimization of the magnetic refrigerator and to determine the related best parameters.

1. Introduction

In 1881 Emil Gabriel Warburg (1846-1931) discovered the magneto caloric effect in an iron sample. It heated a few Millikelvin when moved into a magnetic field and cooled down again when it was removed out of the field (Warburg, 1881). This technology was successfully applied in low temperature physics since the 1930's to cool down samples from a few Kelvin to a few hundreds of a Kelvin above the absolute zero point (-273.15 K).

A milestone - almost comparable to the discovery of the magneto caloric effect by Warburg - was in 1997 the discovery of the «giant» magneto caloric effect (Pecharsky and Gschneidner, 1997a). This publication and some following one's by these authors (Pecharsky and Gschneidner, 1997b) and also of Tegus *et al.* (2002), are responsible that since the beginning of this millennium magnetic refrigeration started to reveal a realistic potential for commercial room temperature applications at least for certain suitable market segments.

Nowadays the literature on the field consists of a majority of studies dealing with the magneto caloric effect (MCE) in materials. Also an increasing number of articles treat thermo-magnetic machine design and calculation, and a somewhat smaller number describes theoretical and numerical simulation work (see e.g. Kitanovski *et al.* (2005) and Šarlah *et al.* (2007).

For example, a thermodynamic model and related numerical simulations of the behavior of a machine with a magneto caloric wheel have been worked out by Egolf *et al.* (2006). Temperature mappings are obtained for both, material and fluid components of the rotor. Engelbrecht *et al.* (2007) used a NTU method to elaborate a full model on the prototype being a liquid AMRR system, with a particle bed built by the Astronautics Corporation of America. They compared the simulation results with experimental data of Zimm *et al.* (2007). An over prediction of loss is shown at low ratio of the thermal capacity of the flowing fluid to the thermal capacity of the matrix. A 1-d "dynamical model" of an active magnetic regenerator has been proposed with the purpose to make a parametric investigation (Tagliafico *et al.* 2009). It was found that parameters could be tuned to obtain an optimal behavior for a given span of the investigated system.

2. Magnetic refrigerator

Rotary magnetic machines work like rotary heat recovery machines applied with success for decades in air conditioning.

A first step is the magnetization of a porous solid magneto caloric structure in a magnetic field, followed by a simultaneous heating-up of the material. By a fluid flow this structure is cooled, and after that it turns out of the magnetic field and shows a demagnetization process. Here the magneto caloric alloy becomes cold and is heated by a fluid, which preferable has the opposite flow direction to the first flow. If the hot fluid on one side is used, it's a heat pump application; if the cold fluid is applied then the machine is a cooler or a refrigerator.

In Figure 1 a magnetic assembly with a porous magneto caloric wheel containing two regions of intense magnetic field and two regions of low magnetic field is presented.

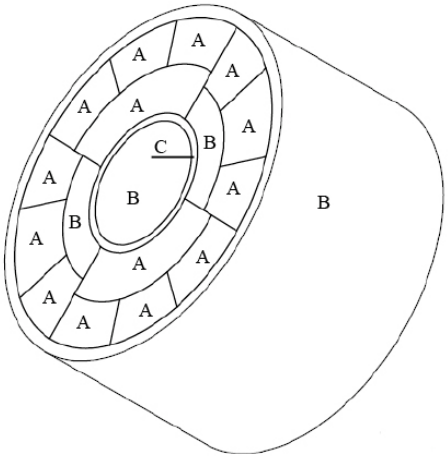

Figure 1: A conceptual drawing of an axial magnetic refrigerator is shown. It contains standard NdFeB magnets (denoted by A) and auxiliary elements for a convenient conduction of the magnetic flux (ferrocobalt, denoted by B) and the turning magneto caloric ring denoted by C (from Swinnen, 2009).

Results of a three-dimensional finite-element numerical simulation, obtained with the ANSYS software, of the magnetic flux density in the magnetic assembly (shown in Figure 1) are shown in Figure 2.

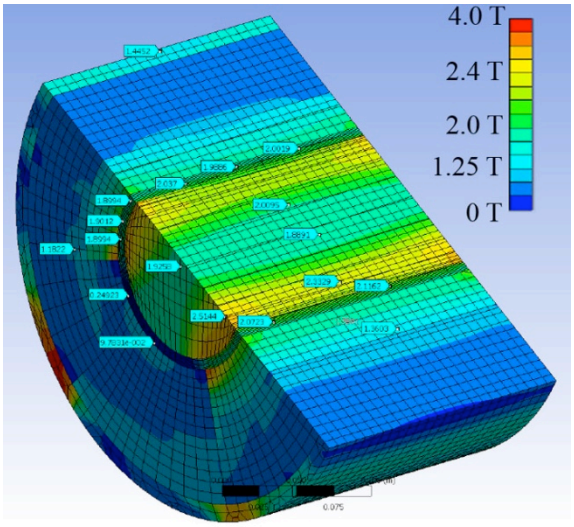

Figure 2: The magnetic field strength distribution in the unit of an induction (Tesla) is shown. The results have been taken from Swinnen, 2009.

3. The theoretical maximum specific cooling power

Essential information for a design and analysis of a magnetic refrigerator is the cooling capacity of the magneto caloric material. The maximum specific cooling energy of a magneto caloric material (see Figure 3) is directly related to the entropy and temperature change, which occurs due to a magnetization/demagnetization of the magneto caloric material. To obtain a maximum cooling capacity, a well-defined domain around the Curie temperature T_C has to be taken into consideration.

The maximum specific cooling energy of a single material is obtained by an isothermal demagnetization at Curie temperature (see Eq. (1)), while the maximum temperature change is obtained by an adiabatic magnetization also at Curie temperature:

$$q_{R\max} = T_C \, \Delta s(T_C) \qquad (1)$$

The $\Delta s(T_C)$ presents the total entropy change at Curie temperature. The maximum specific cooling energy is obtained only with cycles, as e.g. the Ericsson (two isomagnetic field processes, two isothermal processes) or the Stirling (two isomagnetic field processes, two isothermal processes) by also applying a regenerative process. The Carnot cycle cannot perform a so large specific cooling energy compared to the two above described cycles. The same is valid for the Brayton cycle (two isomagnetic field processes, two isentropic processes).

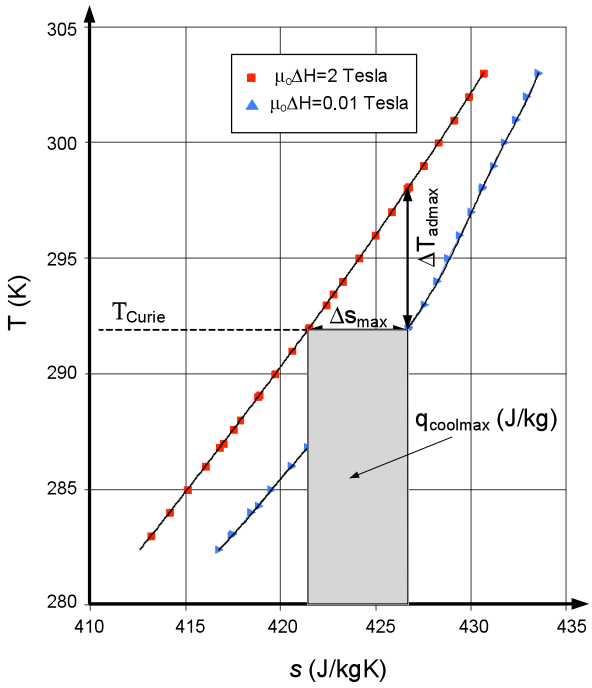

Figure 3: Theoretical maximum specific cooling energy as a result of the isothermal demagnetization process for the rare earth gadolinium is shown in a shaded area (from Egolf *et al*, 2008).

With the frequency of a machine it is possible to define the theoretical maximum specific cooling power as follows:

$$\dot{q}_{R\max} = T_C \, \Delta s(T_C) \, f \qquad (2)$$

The specific cooling power of magneto caloric material may be large even for low magnetic field changes (see Figure 4). However, high frequencies require a fast convective and diffusive heat transfer process. Convective transport is dependent on the fluid flow characteristics as well as on the geometry of the magneto caloric structure. Diffusion does not

present a serious limitation, if small structured magneto caloric material is applied, because the diffusion transport time decreases with the second power of the transport length (Egolf *et al.*, 2006).

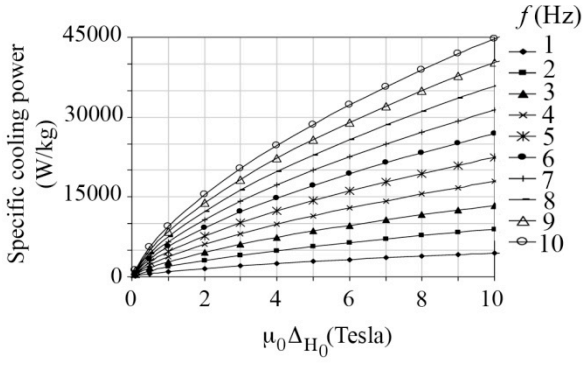

Figure 4: The theoretical maximum specific cooling power for gadolinium as a function of the magnetic field strength variation and the frequency of operation (from Kitanovski and Egolf, 2009).

The fluid friction losses rapidly increase with the frequency of operation, because a characteristic transport time of a fluid lump through the material bed has to be much smaller than the period of rotation. Because small magnetic field changes cause small temperature differences in the material, the magnetic refrigerator usually must operate with a regenerative cycle (or a cascade system). This leads to additional irreversibility's due to the larger number of occurring heat transfer processes and related fluid friction losses. Therefore, it is a wrong opinion that small magnetic fields with high frequencies may be equivalent to high magnetic fields with low frequencies in order to obtain the same temperature span and keeping the same efficiency of a magnetic refrigerator.

Figure 5 shows the comparison of the *COP* of a rotary magnetic household refrigerator (magnetic flux density 2 Tesla) with one containing a hermetic compressor. The heat source temperature is identical to the evaporation temperature of the refrigerant. The thick line corresponds to the *COP* of a Danfoss hermetic compressor (LBP/ MBP and MBP/HBP, R404a/R507, type FR 6CL) with a condensing temperature at 45 °C.

These results show that the frequency of operation depends on the characteristics of a magnetic refrigerator. The reason for this is that a higher velocity of the working fluid leads to a higher-pressure drop and, therefore, also to higher irreversibility's.

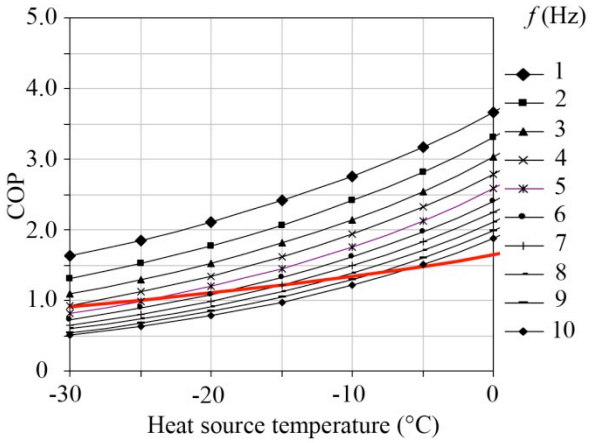

Figure 5: The *COP* of a magnetic household refrigerator as a function of the heat source temperature and the frequency of operation for a magnetic flux density change of 2 Tesla is shown (from Kitanovski *et al.*, 2008). The sink temperature has been fixed at 45 °C. The porosity of the magneto caloric wheel is 10 %.

Figure 5 shows that a magnetic household refrigerator is competitive to one containing a compressor. This is especially the case when the frequency is low, e.g. below 5 Hz; however, for a high magnetic flux density change the frequency may be higher. This leads to a smaller mass and volume of the device, which is very essential mainly because of economic reasons.

4. Physical modeling of the magneto caloric generator

The physical modeling of a rotating porous rotor made of magneto caloric material is described in detail in an earlier article by Kitanovski *et al.* (2005). It

is based on two main simplifying assumptions:

1) The rotation frequency *f* of the ring is low compared to the inverse characteristic time of residence of a fluid lump flowing vertically or horizontally through the porous structure.

2) The heat conduction through the rotor in axial direction is negligible compared to the heat flux by convection.

The magneto caloric porous ring has been divided into two principal kinds of cells, as it is shown in Figure 6.

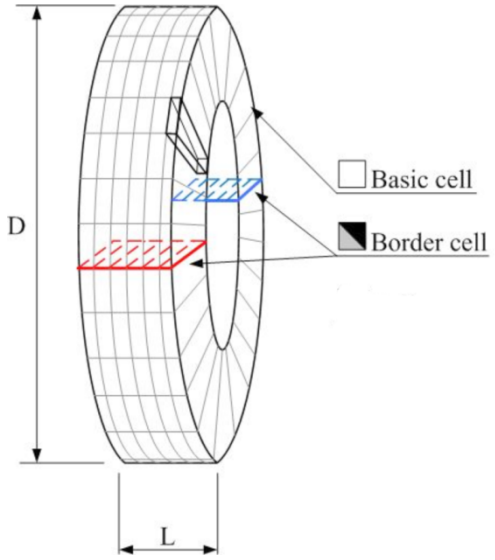

Figure 6: The main center part of a magnetic cooling machine consists of a rotating porous magneto caloric ring. The half top section is in a magnetic field and the half lower section is the zero-field region. In our case two heat transfer fluids flow in opposite axial direction through each of these regions. To show the decomposition of the magneto caloric ring into cells is the main purpose of this figure.

4.1 Basic cells

Basic cells represent physically the part of the magneto caloric rotor and describe the heat transfer by conduction of magneto caloric material and the heat transfer from the fluid to the magneto caloric wheel. Deriving two times two coupled partial differential equations, which are referred to in detail in Kitanovski *et al.* (2005), lead to the following well-conditioned algorithms (3) and (4) for the centre cells:

$$T_{Fout} = (1 - \chi_F)\, T_{Fin} + \chi_F T_{Rin} \tag{3}$$

$$T_{Rout} = (1 - \chi_R)\, T_{Rin} + \chi_R T_{Fin} \tag{4}$$

T denotes the temperature and the index F the Fluid and R the Rotor matrix. The fluid temperature is handed over from an inlet to an outlet in horizontal direction and the rotor temperature identical in the vertical direction. The quantities χ_F and χ_R contain all physical properties of the fluid and the rotor material, respectively, and the heat transfer coefficients. They are defined in equation (5) and (6) as:

$$\chi_R = \frac{\alpha\ \Delta\phi}{\psi\ \delta\ \rho_R\ \omega_R\ c_H} \tag{5}$$

$$\chi_F = \frac{\alpha\ \xi\ \Delta z}{L\ \rho_F\ u_F\ c_{pF}} \tag{6}$$

$\Delta\phi$ and Δz denote the differences in the azimuth and in the axial direction, respectively.

4.2 Border Cells

The virtual elements, describing in time changing sections of the wheel, are related to real physical parts (2-d plans are drawn for their representation (see e.g. in Figure 6)). In the border cells the reversible adiabatic temperature transitions, induced by the alternating magnetic field in the rotor structure, were implemented. The adiabatic temperature change, as a function of the magneto caloric material temperature and the magnetic field change, was determined by mean field theory calculations.

4.3 Programming a Full System

The chosen object-orientated language is Modelica 2.2.1 with the commercialized interface Dymola 6.1. A full description of the computation work can be found in Vuarnoz *et al.* (2009). The assembly of home-made cells (basic cells, border cells) together with numerous standard modules, e.g. for pumps, heat sources and flowPorts, from the thermal "FluidHeatFlow" library, can be assembled to obtain a magneto caloric generator module. As an example, a refrigerator with two magneto caloric generators coupled in a cascade – as shown in Figure 7 – is at present investigated.

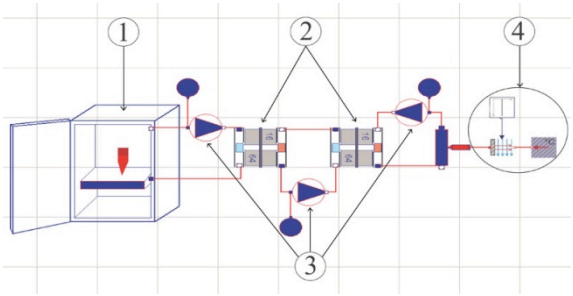

Figure 7: Schematic design of a magnetic refrigerator as implemented into the software Dymola. The main components of the system are: 1) Insulated fridge, 2) Magneto caloric generators, 3) Pumps, 4) Hot heat exchanger, cooled by natural convection of ambient air.

In order to test the manufactured tool, some non-optimized parameters have been chosen (see Appendix 1). The two stages of the cascade process are actually identical and made of 536 g of gadolinium with a porosity of 70 %. An external magnetic field is assumed to have a magnitude of 2 Tesla in the magnetized areas of the porous ring. Air has been chosen to be the working fluid. The mass flow through the porous ring leads to a local velocity in the structure of approximately u_F=2 m/s. The thermal load in the fridge appliance is composed of 10.5 kg chocolate. A full listing of the parameters of the geometry of the porous wheel, grid increment distances and other auxiliary parameters are also presented in Appendix 1.

4.4 Simulation

Temperatures at each inlet and outlet of each generator were monitored. When arriving to their steady states, their values allow the design of a *T-s* diagram of each stage (see Figure 8). The thermodynamic coefficient of performance (*COP*) of each stage can be determined with the help of the *T-s* diagram. This *COP* does not comprise losses by eddy currents and assumes a fully reversible magneto caloric effect.

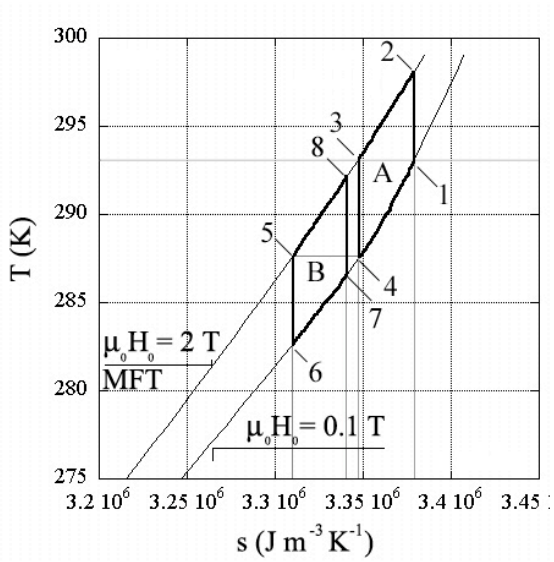

Figure 8: Representation of two Brayton cycles in a temperature versus specific entropy (*T,s*) diagram. It is worked out for gadolinium and has been determined with the mean field theory (MFT). The symbol $\mu_0 H_0$ represents the intensity of the external magnetic field, which is applied.

In the present case, the thermodynamic *COP* of the first stage is 66 and of the second 60. The second stage is less performing, because it is operating more distant from the Curie temperature of gadolinium than the first one. The efficiency of the full system will be necessarily much lower, because it will take in account efficiencies of every component of the system, e.g. pumps, heat exchangers, etc.

The refrigerator possesses a simple regulation sy-

stem, which guarantees a certain stability of the inside air temperature by an alternating sequence of an "ON" and "OFF" mode, as it is shown in Figure 9. The investigated refrigeration unit with a two-step cascade working with a mass of totally 536 g of Gd cools 10.5 kg chocolate 7 K in approximately 14 hours.

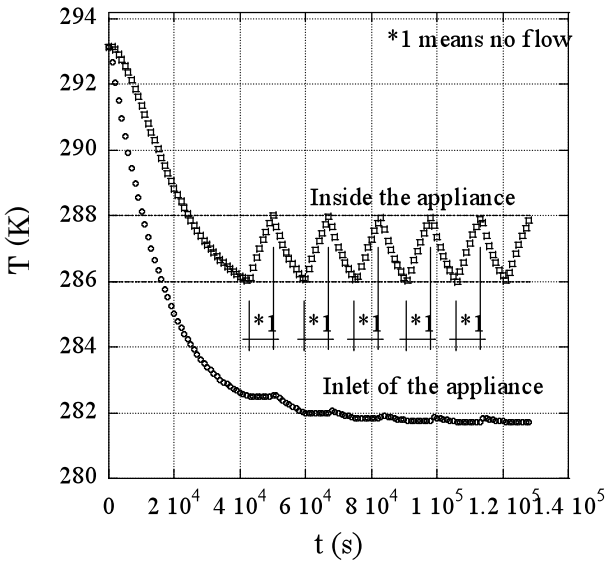

Figure 9: Time evolution of the temperature of the working fluid at the inlet and outlet of the magnetic refrigerator appliance modeled according to the schematic drawing shown in Figure 7. The inlet temperature evolution of the air in the cabinet during the "OFF" mode shows the typical exponential decay as it is expected to occur in such a thermodynamic machine with a thermal inertia and heat transfer losses.

A perfect heat transfer is assumed to occur between the charge and the air in the refrigerator. The inside temperature of the appliance is identical to the one of the air flowing out of the equipment. The refrigerator is assumed to have a standard insulation and no door openings were taken into consideration. The time to reach the steady-state temperature is rather large. The reason is that the thermal charge in the appliance is not in accordance with the mass of the magneto caloric material. However the simulation results are showing the potential of such a developed tool for a parameter study and optimization process. Another kind of system, e.g. regenerative system (see Figure 10) can now easily be implemented for a similar analysis.

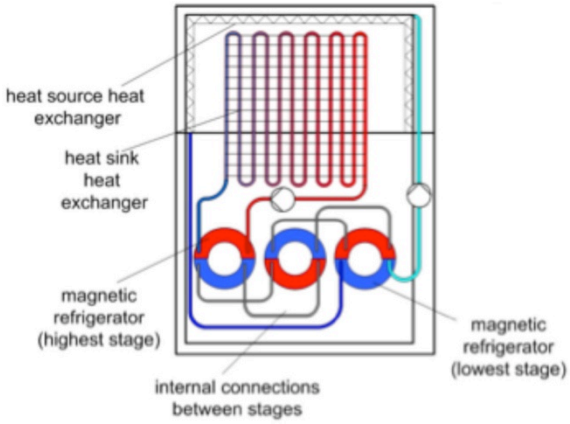

Figure 10: A schematic sketch shows how a three-stage magnetic household refrigerator could be designed. The three red/blue rotor wheels are connected to perform regeneration cycles. Notify that the design may permit to only have two pumps in such a multi-stage machine.

5. Conclusions

In this article magnetic refrigeration is described and a rotary system is investigated. The maximum specific cooling energy that can be extracted from magneto caloric material has been determined. The household refrigerator without a freezing compartment is showing very good prospects for a successful application.

A numerical tool to optimize magnetic refrigerators is presented. It contains a user-friendly commercialized interface Dymola, where by drag and drop methods a refrigerator can be easily built together and modified. Programming in this modern software is performed by the application of the object-oriented language Modelica. The parameters have not yet been determined by solving the numerical method "Optimization Problem", where the parameters are determined in such a manner that a final quantity is optimized. Based on the calculation results, the magneto thermodynamic *T-s* diagram containing the

cycles of the two stages could be reconstructed. Further improvements and the optimizations of this and similar machines are at present under performance.

Acknowledgements

The authors are grateful to the Swiss Federal Office of Energy (Thomas Kopp and Roland Brüniger) for its financial support. We are grateful to the Gebert Rüf Stiftung and the Hes-so foundation for continuous interest in our work.

References

1) Warburg E.: Ann. Phys., vol. **13**, p.141–164 (1881).
2) Pecharsky V.K., Gschneidner K.A. Jr.: "Giant magnetocaloric effect in Gd5(Si2Ge2)", Phys. Rev. Lett. **78** (23) pp. 4494-4497 (1997a).
3) Pecharsky V.K., Gschneidner K.A., Jr.: "Effect of alloying on the giant magneto caloric effect of Gd5(Si2Ge2)", J. Magn. Magn. Mater. **167**, pp. L179-L184 (1997b).
4) Tegus O., Brück E., Buschov K.H.J. De Boer F.R.: "Transitional-metal-based magnetic refrigerants for room-temperature applications", Nature **415**, pp. 150-152 (2002).
5) Kitanovski A., Egolf P.W., Gendre F., Sari O., Besson Ch.: "A rotary heat exchanger magnetic refrigerator". Proceedings of the First Int. Conf. on Magnetic Refrigeration at Room Temperature, (Editor P.W. Egolf), ISBN 2-913149-41-3, Montreux, Switzerland, pp. 297-307 (2005).
6) Šarlah A., Poredos A.: "Dimensionless numerical model for determination of magnetic regenerator's heat transfer coefficient and its operation". Proceeding of the Second Int. Conf. on Magnetic Refrigeration at Room Temperature, (Editor A. Poredos), ISBN 978-2-913149-56-4, Portoroz, Slovenia, pp. 419-426 (2007).
7) Egolf P.W., Sari O., Gendre F.: "Close- to-Carnot-cycle magnetic refrigerators and heat pumps: Analytical machine design and optimization". Proceedings of the Jubilee XX NMMM (New Magnetic Materials of Microelectronics) Conference, Russian Ass. of Mag., Lomonosov State University, Moscow, 12-16. June, AII-02 (2006).
8) Engelbrecht K.L., Nellis G.F., Klein S.A.: "Comparing modeling predictions to experimental data for AMRR systems". Proceeding of the Second Int. Conf. on Magnetic Refrigeration at Room Temperature, (Editor A. Poredos), ISBN 978-2-913149-56-4, Portoroz, Slovenia, pp 349-357 (2007).
9) Zimm C., Auringer J., Boeder A., Chell J. Russek S., Sternberg A.: "Design and initial performance of a magnetic refrigerator with a rotating permanent magnet". Proceeding of the Second Int. Conf. on Magnetic Refrigeration at Room Temperature, (Editor A. Poredos), ISBN 978-2-913149-56-4, Portoroz, Slovenia, pp 341-347 (2007).
10) Tagliafico G., Scarpa F., Tagliafico L,A.: "Dynamic 1D model of an active magnetic regenerator: a parametric investigation", Proceeding of the Third Int. Conf. on Magnetic Refrigeration at Room Temperature, (Editor P.W. Egolf), ISBN 978-2-913149-67-0, Des Moines, USA (2009).
11) Swinnen T.: "Magnetic refrigeration: Theory and simulation with C++ and ANSYS", Bachelor thesis, University of Applied Sciences of Western Switzerland (2009).
12) Egolf P.W., Kitanovski A., Gonin C., Diebold M., Vuarnoz D.: "Magnetic heating, refrigeration and power conversion", Proceeding of the 12th Int. Conf. on Refrigeration and Air Conditioning, paper ID 2298, Purdue, USA, (2008).
13) Egolf P.W., Gendre F., Kitanovski A., Sari O.: "Machbarkeitsstudie für magnetische Wärmepumpen: Anwendungen in der Schweiz", Schlussbericht des Projektes zuhanden des Bundesamtes für Energie Nr.151017 (2006).
14) Kitanovski A., Vuarnoz D., Diebold M., Gonin C., Egolf P.W.: "Application of magnetic refrigeration and its assessment", Final Report of Project No. 152 191, Swiss Federal Office of Energy (2008).
15) Vuarnoz D., Kitanovski A., Gonin C., Sari O.,

Egolf P.W.: “Modeling of a two-stage magnetic refrigerator with wavy-structured gadolinium heat exchangers”. Int. J. Refrig. **33**, 745-752 (2010).

Nomenclature

B	Magnetic field induction (T)
c	Specific heat capacity (J kg^{-1} K^{-1})
CUP	Chocolate Unit Plate, equiv. 100 g
d	Diameter (m)
f	Frequency (s^{-1})
L	Length (m)
m	Mass (kg)
p	Pressure (Pa)
s	Specific entropy (J m^{-3} K^{-1})
T	Temperature (K)
v	Velocity (m s^{-1})
z	Length (m)

Subscript

ad	Adiabatic
F	Fluid
H	Constant magnetic field
h	Hydraulic
in	Inlet
out	Outlet
R	Rotor

Greek

α	Heat transfer coeff. (W m^{-2} K^{-1})
δ	Characteristic geom. quantity (m)
Δ	Difference
ξ	Characteristic geom. quantity
ρ	Density (kg m^{-3})
υ	Kinematic viscosity (m^2 s^{-1})
ϕ	Angle (°)
χ	Characteristic number (-)
ψ	Porosity (m^3/m^3)
ω	Angular frequency (s^{-1})

Appendix

Appendix 1: Parameters of numerical simulations.

Quantity	Symbol	Value
External diameter (m)	d_0	0.1
Inner diameter (m)	d_1	0.08
Length (m)	L	0.04
Porosity (%)	ψ	30
Density rotor (kg m^{-3})	ρ_R	7900
Frequency rotor (Hz)	f	0.35
Forced heat transfer coeff. Wm^{-2}K^{-1})	α	210
Fictive volume flow rotor (m^{3}s^{-1})	$\dot{V}_R$	0.0028
Intensity low ext. field (T)	H_0	0.1
Intensity high ext. field (T)	H_1	2.0
Hydraulic diameter (m)	d_h	4.67*10^{-4}
Density air (kg m^{-3})	ρ_{Air}	1.149
Kinematic viscosity of air (m^{2}s^{-1})	υ	16.3*10^{-6}
Spec. heat capacity air (J kg^{-1}K^{-1})	c_{pair}	1007
Viscosity rotor loop (m^{2}s^{-1})	υ_R	0
Nb. mesh horizontal (-)	i	16
Nb. mesh vertical (-)	j	64
Intervals (printed) (-)	int	128
Precision (-)	$prec.$	0.001
Integrator step (s)	FIS	0.5
Start time (s)	t_0	0
Stop time (s)	t_{stop}	12800
Thermal resistance rotor (K W^{-1})	R_{tot}	1.0378
Ambient temperature (K)	T_{amb}	293.15
Free convection heat transfer coefficient (Wm^{-2} K^{-1})	α_{Nat}	5
Volume flow (m^3 s^{-1})	$\dot{V}$	0.002
Charge (g)	CUP	100
Spec. heat chocolate (J kg^{-1} K^{-1})	c_{pchoco}	2000
Inner dim. appliance (m)	a*b*c	0.3*0.35*0.4
Initial temperature (K)	T_{ini}	293.15